Molecular photoswitches mediating the strain-driven disassembly of supramolecular tubules

Jean W. Fredy[a,b,1], Alejandro Méndez-Ardoy[a,1], Supaporn Kwangmettatam[a,b,1], Davide Bochicchio[c], Benjamin Matt[b], Marc C. A. Stuart[d], Jurriaan Huskens[a], Nathalie Katsonis[b], Giovanni M. Pavan[c,2], and Tibor Kudernac[a,2]

[a]Molecular Nanofabrication Group, MESA+ Institute for Nanotechnology, University of Twente, 7500 AE Enschede, The Netherlands; [b]Bio-inspired and Smart Materials, MESA+ Institute for Nanotechnology, University of Twente, 7500 AE Enschede, The Netherlands; [c]Department of Innovative Technologies, University of Applied Sciences and Arts of Southern Switzerland, CH-6928 Manno, Switzerland; and [d]Faculty of Mathematics and Natural Sciences, Groningen Institute of Biomolecular Sciences and Biotechnology, University of Groningen, 9747 AG Groningen, The Netherlands

Edited by Thomas E. Mallouk, The Pennsylvania State University, University Park, PA, and approved September 12, 2017 (received for review June 21, 2017)

Chemists have created molecular machines and switches with specific mechanical responses that were typically demonstrated in solution, where mechanically relevant motion is dissipated in the Brownian storm. The next challenge consists of designing specific mechanisms through which the action of individual molecules is transmitted to a supramolecular architecture, with a sense of directionality. Cellular microtubules are capable of meeting such a challenge. While their capacity to generate pushing forces by ratcheting growth is well known, conversely these versatile machines can also pull microscopic objects apart through a burst of their rigid tubular structure. One essential feature of this disassembling mechanism is the accumulation of strain in the tubules, which develops when tubulin dimers change shape, triggered by a hydrolysis event. We envision a strategy toward supramolecular machines generating directional pulling forces by harnessing the mechanically purposeful motion of molecular switches in supramolecular tubules. Here, we report on wholly synthetic, water-soluble, and chiral tubules that incorporate photoswitchable building blocks in their supramolecular architecture. Under illumination, these tubules display a nonlinear operation mode, by which light is transformed into units of strain by the shape changes of individual switches, until a threshold is reached and the tubules unleash the strain energy. The operation of this wholly synthetic and stripped-down system compares to the conformational wave by which cellular microtubules disassemble. Additionally, atomistic simulations provide molecular insight into how strain accumulates to induce destabilization. Our findings pave the way toward supramolecular machines that would photogenerate pulling forces, at the nanoscale and beyond.

artificial molecular switches | supramolecular polymers | supramolecular machines | light

Essentially all motion in living organisms emerges from the collective action of molecular machines transforming chemical energy into ordered activity. Inspired by nature's machinery, chemists have moved from building static molecular structures to designing and synthesizing molecules that display mechanically relevant motion (1, 2), such as molecular switches (3, 4), pincers (5), motors (6–8), pumps (9), shuttles (9, 10), muscles (11), walkers (12), robotic arms (13), artificial peptide synthesizers (14), and self-propelled molecular cars exhibiting directional motion (15). The operation of these small molecules has been studied in solution primarily, where any mechanical action is overwhelmed by random Brownian motion.

Remarkably, nature's molecular machines also operate in a liquid environment, where despite the Brownian storm and the constant flux of building blocks they generate strong directional forces (16) and synthesize essential molecules (17). Two characteristics underpin evolutionary designs: first, nonequilibrium operation of supramolecular machines is maintained by constant influx of chemical fuels and second, these machines are integrated into even larger supramolecular assemblies such as filaments, membranes, or tissues, to guide and coordinate the overall operation against the Brownian storm.

Reaching this remarkable level of functionality in artificial systems requires strategies where mechanically purposeful molecular motion can be transmitted effectively into motion at the supramolecular level—a challenge that has thus far proven elusive.

Cellular microtubules are versatile supramolecular machines that are capable of producing two types of directional forces under continuous influx of energy: they pull chromosomes apart through catastrophic disassembly, and shape-shift cells as they grow using chemical energy (18). This capacity to produce forces efficiently is inherently encoded into their supramolecular architecture: microtubules are in essence stiff cylinders that are self-assembled from molecules that undergo chemically fueled conformational switching between assembling and nonassembling forms (19). Although the functional disassembly of cellular microtubules is still not understood fully, it appears that conformational changes in the tubules' building blocks induce a strain that builds up and releases abruptly to produce a directional mechanical force upon disassembly (20), a process that has been described theoretically by the conformational wave model (21, 22).

Here, we report the creation of synthetic supramolecular tubules in which the structural change at the level of individual building blocks is controlled by photochromic switching, which

Significance

Developing molecular machines has been a leading goal for scientists, but to be practically valuable their mechanically relevant motion must be decoupled from the Brownian storm that dominates in solution. The disassembly of cellular tubules operates by the switching of the shapes of the building blocks, ultimately pulling sets of chromosomes apart. Here, we show that artificial photoswitches can be incorporated within supramolecular microtubules and that individual switching events lead to conversion of light into elastic energy that can be stored, accumulated, and subsequently released to produce a mechanical effect. The work paves the way toward fully artificial supramolecular machines that convert molecular motion into sophisticated operation modes, at length scales that are typically the realm of living matter.

Author contributions: J.W.F., A.M.-A., and S.K. performed research; B.M. contributed new reagents/analytic tools; J.W.F., A.M.-A., S.K., D.B., M.C.A.S., J.H., N.K., and T.K. analyzed data; D.B. performed the simulations; M.C.A.S. performed the cryo-TEM experiments; G.M.P. designed and supervised the modeling work; T.K. designed and supervised the research; and N.K., G.M.P., and T.K. wrote the paper.

The authors declare no conflict of interest.

This article is a PNAS Direct Submission.

See Commentary on page 11804.

[1]J.W.F., A.M.-A., and S.K. contributed equally to this work.

[2]To whom correspondence may be addressed. Email: giovanni.pavan@supsi.ch or t.kudernac@utwente.nl.

This article contains supporting information online at www.pnas.org/lookup/suppl/doi:10.1073/pnas.1711184114/-/DCSupplemental.

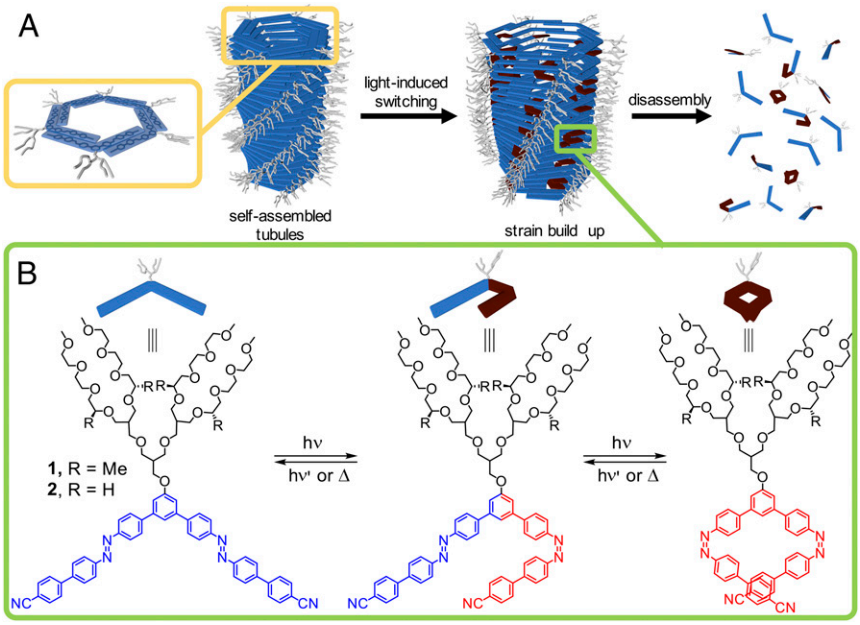

Fig. 1. Concept of strain buildup disassembly of synthetic supramolecular tubules and molecular design of the building blocks. (*A*) Disassembly of synthetic tubules by light. Hydrophobic interaction, π–π stacking, and shape recognition drives the spontaneous assembly of the stable building blocks into supramolecular tubules in water. Light-triggered *trans*-to-*cis* isomerization within the hydrophobic part causes shape changes and eventually disassembly of the tubular structure. (*B*) Chiral building block (**1**) incorporating (*S*)-stereocenters in its hydrophilic moiety and its achiral counterpart (**2**). Notably, the chirality of building blocks has been proven to influence equilibrium dynamics of supramolecular assemblies dramatically (40). Upon irradiation with UV light (λ = 365 nm), the building block undergoes *trans*-to-*cis* isomerization (not all possible conformations are displayed on this scheme). The *trans*/*cis* ratio at photostationary state is ~30/70 (*SI Appendix*, Fig. S5). The reverse *cis*-to-*trans* switching can be realized thermally (with a half-life of *ca*. 12 h at 20 °C), or by irradiation with visible light (*SI Appendix*, Fig. S6).

contributes to pushing the system gradually toward higher energy states, and eventually induces its catastrophic disassembly (Fig. 1*A*). Light constitutes an ideal source of energy that can be supplied continuously to an isolated system to obtain structural switching—as opposed to previously employed external environmental triggers that do not modify the structure of the building blocks [i.e., salinity (23) and temperature (24)]. Notwithstanding the tubular shape, a number of pioneering reports on supramolecular fibers (25, 26) have demonstrated strategies to achieve out-of-equilibrium operation (27–30). The mechanism of assembly of supramolecular polymers, mostly fiber-like objects, has attracted much attention (31, 32), but much less is known about the mechanism by which these fibers disassemble (29). In addition to the presence of a hollow cavity core that is intrinsic to a tubule (33), a major difference between supramolecular tubules and fibers lies in the rigidity of the tubules versus the flexibility of the fibers. Consequently, from a dynamic point of view, synthetic tubules can be expected to exhibit a much slower exchange rate between building blocks in solution and building blocks in the tubule, which also substantially impacts their disassembly mechanism. Herein we describe how these molecular specificities can be encoded into a complex supramolecular system that operates in water and demonstrate that this strategy results in a nonlinear, three-step mechanism that mimics the conformational wave disassembly of cellular microtubules (22).

Results and Discussion

Molecular Design. The use of water as a solvent requires the engineering of photoresponsive building blocks that spontaneously self-assemble in water. Our design involves a V-shaped aromatic core in which two azobenzene photoswitches are incorporated as shape-changing activators (Fig. 1*B*). The V-shaped core is connected to branched hydrophilic oligoether chains that help solubilize the molecules in water and imbues them with an amphiphilic character. In the absence of UV light, the planar *trans* form is present, and the self-assembly of the building blocks into tubes is thus expected to be driven by the combination of hydrophobic effects, π–π interactions and shape recognition, as has been reported for other shape-persistent building blocks (23, 24, 34). In contrast, the *cis* form disrupts both planarity and the V shape of the hydrophobic part and our design thus builds on the concept that *trans*–*cis* isomerization should promote switching between the assembling and nonassembling forms of the building blocks (Fig. 1).

Self-Assembly of Synthetic Tubules in Water. In water, both building blocks **1** and **2** form noncovalent hexameric macrocycles that stack on top of each other to form tubules (Fig. 1*A*), as manifested in the elongated architectures observed in the transmission electron micrographs (Fig. 2*A* for **1**, and *SI Appendix*, Fig. S7*C* for **2**). Atomic

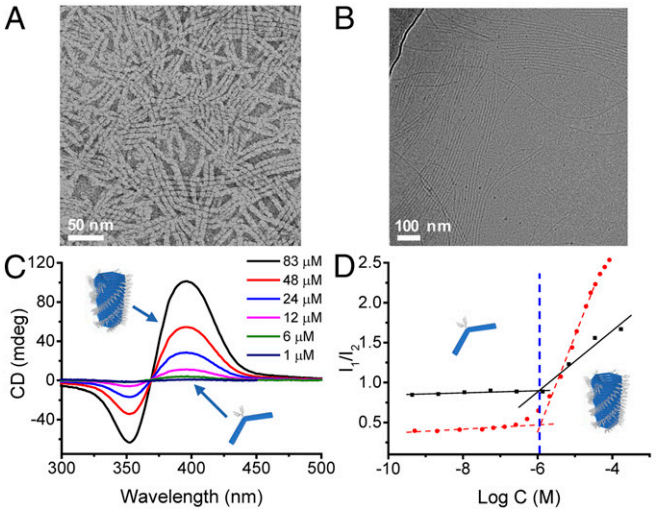

Fig. 2. Synthetic tubules spontaneously form in water. (*A*) TEM micrograph of the tubules formed by building block **1** at c = 83 μM. (*B*) Cryo-TEM micrograph of the tubules formed by building block **2** (1.3 mM). The main cryo-TEM contrast is provided by the core of the tubules constituted by the aromatic units. (*C*) CD spectra at incrementally increased concentrations of **1** between 1 μM (absence of the CD signal) to 83 μM (the highest CD intensity). (*D*) Determination of the critical aggregation concentration for building blocks **1** and **2** using the fluorescent probe Nile red (0.94 μM). The ordinate shows the ratio of intensities of the fluorescence bands (612 and 650 nm for **1**; 621 and 647 nm for **2**) (red dots, **1** and black square, **2**). Nile red present in the hydrophobic environment of the tubules shows increased fluorescence intensity and an emission maximum at λ_{max} ~ 620 nm compared with λ_{max} ~ 650 nm in water (*SI Appendix*, Fig. S11).

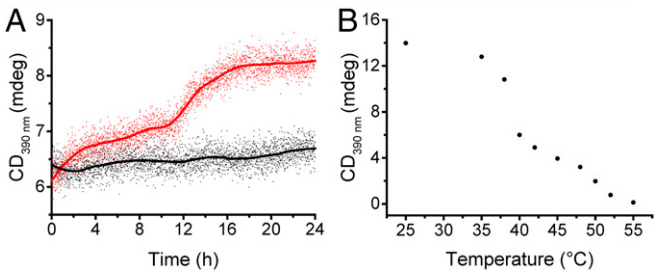

Fig. 3. The preformed supramolecular tubules remain in an out-of-equilibrium kinetic trap. (*A*) We monitor the evolution of the CD signal after mixing a 1:1 ratio of preformed chiral tubules from **1** (2.5 μM) and preformed achiral tubules from **2** (2.5 μM) and compare the dynamic behavior in either pure water (black line) or in water/acetonitrile 95/5 (red line). Over 24 h, chiral amplification is apparent in water/acetonitrile and is translated into a gradual increase of CD signal, which indicates that the chiral and achiral building blocks are mixing to form a larger number of chiral tubes (i.e., the system displays a sergeants and soldiers effect). In stark contrast, chiral amplification is not observed in water. The absence of chiral amplification indicates that in water exchange between the building blocks, which the tubules are composed of, does not occur. These data indicate that in water and over the timescale of the measurements, the structure of the tubules is kinetically trapped at room temperature. (*B*) CD signal of **1** recorded at λ = 390 nm in water (2.5 μM), for varying temperatures.

force microscopy (AFM) also confirms these findings (*SI Appendix*, Fig. S8). Cryo-TEM images reveal the internal aromatic part of the tubules with the uniform size along its whole length (Fig. 2*B*). The measured diameter (d ≈ 5 nm) corresponds to the expected diameter of the hexamer (*SI Appendix*, Fig. S9). The periodicity of bundled tubules indicates the external diameter of the tubule is *ca*. 11 nm, in agreement with the value estimated from molecular models (*SI Appendix*, Figs. S9 and S10). TEM micrographs indicate an external diameter of *ca*. 7 nm for both **1** and **2** (*SI Appendix*, Fig. S7), which we attribute to a difference in sample preparation; when out of solution the hydrophilic chains interdigitate partially upon drying.

The structural information provided by microscopy is complemented by spectroscopic data. Upon self-assembly of **1** in water, a CD signal appears with a zero-crossing point that corresponds to the λ_{max} of the azobenzene chromophores. The intensity of the CD signal increases with the concentration of **1**, indicating that **1** assembles into tubules with a preferred handedness (Fig. 2*C*). The shape of the CD spectrum remains constant between 1 μM and 83 μM, which indicates that the supramolecular structures are robust and uniform. A CD signal is not observed over the same concentration range when **1** is dissolved in acetonitrile, which indicates that molecular tubes do not form in acetonitrile. Achiral building block **2** does not yield a CD signal in water, which we attribute to the formation of tubules without preferential handedness.

Effective control over the dynamics of the synthetic tubules was achieved close to the critical aggregation concentration, where small changes in concentration can drive substantial changes at the supramolecular level. The critical aggregation concentration was determined by plotting changes in the fluorescence of a probe (Nile red) that favors hydrophobic cavities (35), for increasing concentrations of building blocks, and was found to be ∼1 μM (Fig. 2*D* and *SI Appendix*, Fig. S11).

Synthetic supramolecular architectures are dynamic in nature and, to date, their design has been such that they readily adapt to changing boundary conditions. As soon as the conditions change, the rapid exchange between the assembled building blocks and the isolated building blocks secures a fast reequilibration process. In contrast, we anticipated that if the exchange between the assembled building blocks and those in solution is slowed, then the architectures will display a tendency to linger out of equilibrium, in a higher energy state. Nature's supramolecular machines have evolved in such a way that they can operate out of equilibrium and employ this higher energy state to perform useful tasks. To examine the exchange rate between building blocks forming the tubules and those in solution, we mixed two populations of the individually preformed tubules formed by chiral **1** and achiral **2**. Upon mixing an aqueous solution of the chiral tubules **1** with another aqueous solution containing tubules **2** the CD signal remained constant for 24 h (Fig. 3*A*). In contrast, upon mixing the same tubules in water/acetonitrile (95/5) the CD signal increased and revealed amplification of chirality, an effect known as the sergeants and soldiers principle (36). These data indicate that in water the exchange of molecules between the tubules and the solution is slow. In contrast, this exchange is fast in the water/acetonitrile mixture, likely because of the higher solubility of all building blocks in acetonitrile.

Further insight into the equilibrium dynamics of the tubules formed by **1** can be extracted from the temperature dependence of the CD spectra. Overall, the intensity of the CD signal recorded at λ = 390 nm decreases with an increasing temperature, until it completely disappears at 55 °C (Fig. 3*B*). The disappearance of the CD signal most likely originates from the greater thermal energy that decreases the average length of the tubules until they become soluble. While at temperatures between 40 °C and 55 °C the CD signal decreases linearly, below

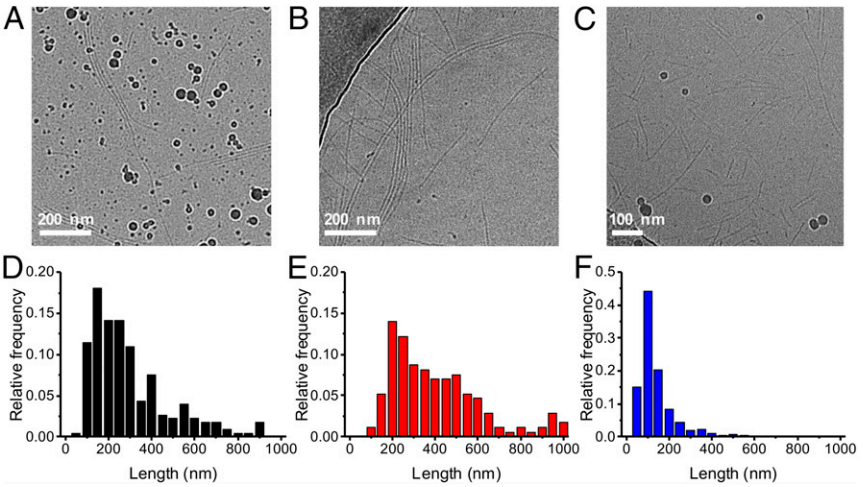

Fig. 4. Structural evolution of the synthetic tubules formed by **2** upon irradiation with light. (*A*) Cryo-TEM picture before UV irradiation, (*B*) after 20 min of irradiation, (*C*) and after 60 min of irradiation in water (λ = 365 nm, c = 1.33 mM). The darker spherical objects are artifacts from the cryogenic medium. (*D*) Length distribution before UV irradiation (over 230 tubules), (*E*) after 20 min of UV irradiation (over 170 tubules), and (*F*) after 60 min of UV irradiation (over 800 tubules).

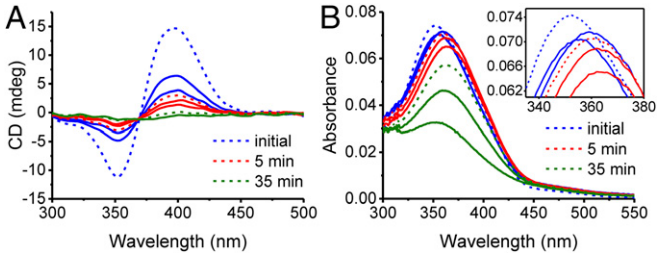

Fig. 5. Conversion of light into molecular and supramolecular strain. (*A*) Evolution of the CD spectra of tubules formed by **1** (2.5 μM solution of **1** in water) as a function of the time upon irradiation (measured at 0, 1, 2, 5, 10, 20, 35, 50, and 60 min) with UV light (λ = 365 nm). The disappearance of the CD signal after 35 min indicates that the tubules have disappeared. (*B*) Absorption spectral changes induced by irradiation with UV light.

40 °C the system starts exhibiting a nonlinear behavior. Between 25 °C and 35 °C the intensity of the CD signal decreases by less than by 10%, whereas between 35 °C and 40 °C the CD signal abruptly reduces by 50%. This shows that the assembled tubules are kinetically trapped around room temperature within the timescale of the measurements, whereas at elevated temperatures the structure dynamically adapts to temperature changes. Although the response of the self-assembled tubules to temperature cannot be directly compared with the situation when the system responses to structural changes of the building blocks, it gives a valuable insight into the dynamics of the molecular exchange between the assembled and free state. Overall, we conclude that at ambient temperature the system of tubules formed in a purely aqueous environment has the tendency to linger out of equilibrium after it has been disrupted.

Conversion of Light into Supramolecular Strain. Next, we studied the dynamics of the synthetic tubules under a continuous influx of energy, through irradiation with light. The azobenzene units in the aromatic core of the building blocks provide the light-responsive trigger for the disassembly. In acetonitrile, where tubules are not formed, we verified that the azobenzene unit displays the expected photoswitching behavior, in both building blocks **1** and **2** (*SI Appendix*, Fig. S6). Upon irradiation of the *trans* form with UV light (λ = 365 nm), *trans*-to-*cis* isomerization occurs. These large geometrical changes are altering planarity and conjugation, and therefore they are manifested in a decrease of the π–π* absorption band at λ_{max} = 367 nm and a less pronounced increase of the n–π* absorption around 450 nm.

Illumination of the tubules (**2**, 1.33 mM) for less than 20 min did not yield a significant change in either their length (Fig. 4 *A* and *B*) or diameter (increased by ∼1 nm, *SI Appendix*, Fig. S12). The marginal increase in length falls within the experimental uncertainty. Further, there are always 1 μM of nonassembled building blocks in solution (as indicated by the value of the critical aggregation concentration before irradiation), but their low number cannot account for this marginal length increase at a concentration of 1.33 mM.

After 60 min of irradiation, cryo-TEM images show that the tubules become shorter (Fig. 4*C*) and that their number increases (*SI Appendix*, Fig. S13). The distribution in length shows the presence of shorter tubules after 60 min of UV irradiation with the disappearance of long tubules (>300 nm) compared with the distribution before irradiation or after irradiation for 20 min (Fig. 4 *D*–*F*). Combined, these observations indicate that the tubules break into shorter segments, tentatively at positions where the azobenzene groups are switched to the *cis* form. Dynamic light scattering (DLS) data obtained in situ, at lower concentrations, support this conclusion further (100 μM, *SI Appendix*, Fig. S14). At concentrations of ∼1.33 mM used in the cryo-TEM measurements, complete disassembly of the tubules was not observed, as the remaining concentration of the *trans* form at the photostationary state is considerably greater than the critical aggregation concentration.

At lower concentrations of **1** in water (2.5 μM), full disassembly is achieved (Fig. 5*A*). Parallel monitoring of the disassembly process by CD and by UV-visible (UV-vis) absorption spectroscopy shows that the complete disassembly is achieved after 35 min of irradiation, that is, before a photostationary state is reached (Fig. 5*B*), with the *trans*/*cis* ratio reaching 83/17 only (*SI Appendix*, Fig. S15).

The photo-triggered decrease in the CD signal does not follow a monoexponential behavior (Figs. 5*A* and 6*A*). Instead, 80% of the CD signal is lost abruptly within the first minutes of irradiation, when only 7% of the *trans* form has switched into the *cis* form. We attribute this first phase to a reduction of the helical twist, which is accompanied by a red shift of the wavelength of maximum absorbance λ_{max} (Figs. 5*B* and 6*B* and *SI Appendix*, Fig. S16). Such a red shift indicates a change toward another molecular organization (J-aggregates) (37), leading us to conclude that the building blocks slide with respect to each other, within the tubules. After 5 min, when the *trans*/*cis* ratio is estimated at 93/7, the λ_{max} reaches its maximum value and remains constant for a further 30 min of irradiation (Figs. 5*B* and 6*B*). During this time, the CD signal continues to decrease, albeit at a slower rate. After 35 min of irradiation, the λ_{max} starts to shift

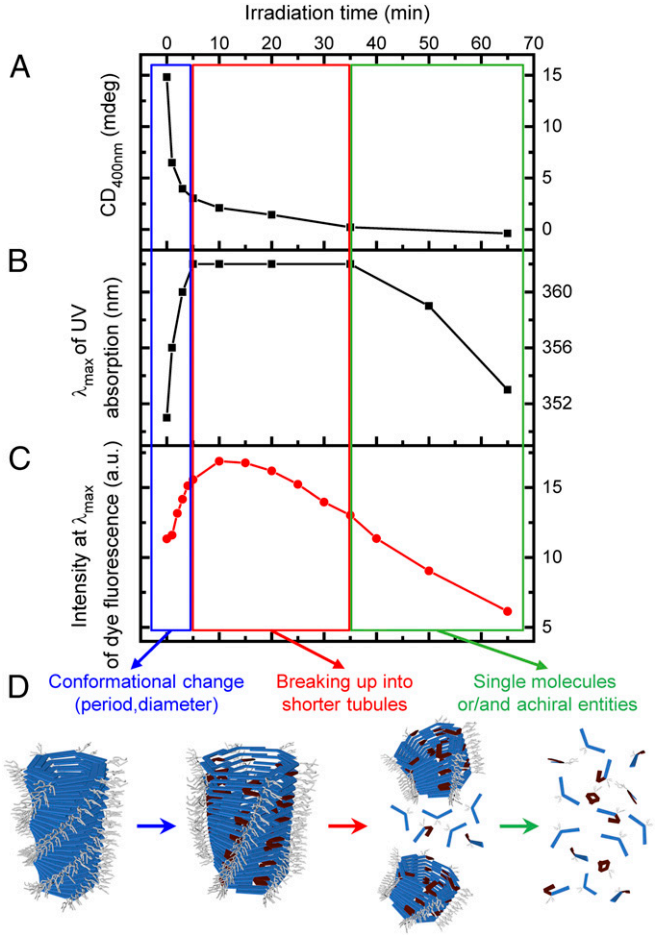

Fig. 6. Proposed mechanism for the light-triggered disassembly of synthetic tubules in water. (*A*) CD intensity at λ = 400 nm and (*B*) position of λ_{max} during the light-triggered disassembly in water (2.5 μM of **1** in water). (*C*) Fluorescence intensity of Nile red (0.94 μM) at λ_{max} during the light-triggered disassembly of tubules formed by **1** in water (2.5 μM). (*D*) Scheme showing the stepwise mechanism of disassembly in water. Strain energy accumulates until it induces explosive breakage of the tubules.

toward shorter wavelengths, while the CD signal approaches zero. Once irradiation stops, the building blocks undergo thermal *cis*-to-*trans* switching (*SI Appendix*, Fig. S6); however, full reversibility of the supramolecular system is not achieved in these experimental conditions, likely because constant recovery of the *trans* form does not mediate the same cooperative effects as in a situation that involves the *trans* form exclusively.

When Nile red (0.94 μM) is encapsulated in the tubules formed by **1** in water (2.5 μM), the changes in UV-vis absorbance and CD spectra upon irradiation are the same as in the absence of the fluorescent probe (*SI Appendix*, Fig. S17), which indicates that the encapsulation of the Nile red does not alter the photo-triggered disassembly pathway. Release of Nile red expected to occur alongside the disassembly of the tubules reflects the complex disassembly process. The release of Nile red is manifested in changes in fluorescence. During the first minutes of irradiation the intensity of the fluorescent signal increases (Fig. 6*C* and *SI Appendix*, Fig. S17), which indicates an uptake of additional Nile red. A blue shift of the maximum emission wavelength (*SI Appendix*, Fig. S17) corresponds to a reorganization of the hydrophobic cavity, which is consistent with the red shift observed by UV-vis spectroscopy. After the initial increase of intensity, the fluorescent signal starts steadily decreasing (Fig. 6*C* and *SI Appendix*, Fig. S17), which indicates that Nile red is released and the tubules are disassembling.

Insights into the Mechanical Operation of the Tubules. Overall, irradiation of the self-assembled tubules pushes them out of equilibrium and toward a complex stepwise disassembly (Fig. 6). First, when irradiation begins, the *trans* form of the azobenzene switches to the *cis* form at numbers that remain sufficiently low to be stabilized within the tubules, without forcing them to disassemble. The strain induced by the nonplanar and bended *cis* form is balanced by the free energy that would be required to solubilize the *cis* form in water. As irradiation proceeds, the increasing amount of *cis* form gradually builds up further strain. Next, a critical amount of *cis* form within the tubules is exceeded and they start to break up, most likely at places where the concentration of the *cis* form is the highest in the tubules. The breaking of the tubules decreases the effective length of the hydrophobic cavity where the fluorescent probe can be encapsulated, which results in its gradual release and decrease of fluorescence (Fig. 6*C*). Finally, when the tubules become shorter than their critical nucleation size they disappear completely. This final phase of the disassembly comes with a clear blue shift of the λ_{max}, as a sizeable fraction of the molecules are in the *cis* form and consequently start dispersing from the assembled state into individually solubilized molecules. The absence of isodichroic point is in agreement with switching from a CD-active assembly to a CD-inactive solution of molecules.

Our results also show that the exchange rate of the building blocks has a significant impact on the dynamics of the system. Irradiation of the tubules in a water/acetonitrile (95/5) solution is not accompanied by a shift of the absorption band. The CD signal consistently shows a simple behavior (*SI Appendix*, Fig. S18), which indicates that in the presence of an organic solvent the disassembly loses its complexity and follows a simple process, where the initial lag phase and buildup of strain are typically absent.

Alternative mechanisms for the dynamic molecular behavior on which we report can be excluded on the basis that they fail to support experimental evidence, including (*i*) the possibility of slow dissolution of the *cis* form and subsequent reequilibration of the assemblies that would be dictated by a lower concentration of the *trans* form in the system and (*ii*) the hypothesis that *trans*-to-*cis* isomerization would occur at a higher rate at the edge of the tubules, and induce dissolution of the *cis* form. In both cases, the tubules would undoubtedly shorten rather than break and, moreover, fast reequilibration within the timescale of minutes would be required, which clearly does not happen in the current system (Fig. 3). Furthermore, these alternative mechanisms would not account for the observed spectral shifts, nor would the change of solvent alter the observed behavior.

Strain Buildup and Tubule Destabilization Captured by All-Atom Simulations. Atomistic modeling provides further insight into the strain buildup in the tubules. Atomistic models for **1** and for the corresponding equilibrated tubule are shown in Fig. 7 (computational details are provided in *SI Appendix*). Tubule **1** was equilibrated and found very stable during 150 ns of an all-atom molecular dynamics (AA-MD) simulation (*SI Appendix*, Fig. S19). As used recently in the study of molecular transitions in supramolecular polymers (38), starting from equilibrated tubule **1** (Fig. 7*A*) we used well-tempered metadynamics (39) to calculate the minimum energy that is necessary for *trans*-to-*cis* isomerization in a monomer within the tubule (*SI Appendix*, Fig. S20). We used this information to set up out-of-equilibrium AA-MD simulations where *trans*-to-*cis* isomerization could be observed iteratively. The C-N–N-C dihedral angle potential of the assembled monomers was modified to disfavor the *trans* form (*SI Appendix*), and as a result switching to the *cis* form was induced in the course of the simulation. This condition is consistent with all monomers being uniformly irradiated by light, while each transition depends on the crowding around individual monomers.

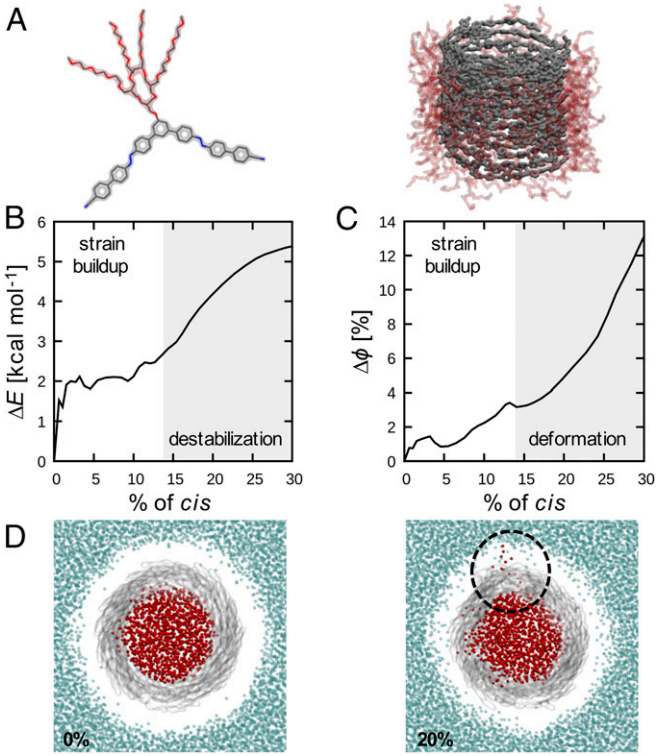

Fig. 7. Strain build-up and tubule destabilization captured by all-atom simulations. (*A*) Atomistic models of building block **1** and of the unperturbed original tubule. (*B*) Energy absorbed by the tubule (Δ*E*, values per-monomer) as a function of the percentage of *cis* form. (*C*) Deviation from the ordered arrangement of the monomers in unperturbed **1** (ΔΦ, in percentage), as a function of the percentage of *cis* form. Data are averaged data from three replica simulations. (*D*) Snapshots of tubule from **1** at the start (0%) and once *trans*-to-*cis* isomerization has reached 20%. Aromatic units are colored gray, internal water molecules are colored red while external water molecules are blue (PEG groups are not shown for clarity; they appear as voids). Above 20% of *trans*-to-*cis* isomerization, water diffuses in and out of holes in the structure (black circle).

During simulations, the azobenzenes were seen to undergo *trans*-to-*cis* isomerization, which allows monitoring of the energy ΔE absorbed by the assembly, as a function of the increasing percentage of *cis* form in the tubule (Fig. 7*B*). ΔE correlates to the strain energy that builds up in the system. The results demonstrate that the accumulation of strain in a tubule is nonlinear. In particular, while below ~10% of *trans–cis* transition we observe an initial phase where the supramolecular structure can keep the ΔE constant (ΔE ~2 kcal·mol^{-1}, average value per-monomer in the system), above ~15% the ΔE rises considerably. Analysis of how much the monomer arrangement in the assembly deviates from the ordered one in the original tubule (Fig. 7*C*, $\Delta\Phi$) shows that structural deformations in the tube are also nonlinear. Globally, the system shows a "stop-and-go" behavior, where the tubule accumulates energy, which is then released as plastic deformations of the structure. In fact, above ~15% of *trans*-to-*cis* isomerization we clearly observe the appearance of holes in the tubule (Fig. 7*D*), which constitutes further evidence of structural collapse.

These simulations are representative of a reduced portion of an infinite supramolecular tubule and are limited to a 100-ns timescale. However, while not allowing us to observe full disassembly of the tubules into monomers during the runs, the model provides evidence of the structural and energetic impairment introduced into the assembly by increasing levels of *trans*-to-*cis* isomerization, which are the key molecular factors underpinning tubule disassembly by exposure to light.

Conclusion. A complex, multistep, light-driven disassembly of aqueous supramolecular tubular assemblies has been demonstrated. The initial conversion of light into tubular strain, which is stored and accumulated before the system breaks apart, is reminiscent of the strain-driven disassembly of cellular microtubules, by which these biological machines generate forces that pull chromosomes apart—another challenge is to combine this operation mode with their complementary operation mechanism, where they push objects by ratcheting upon growing. Here, the strain energy that accumulates during the initial phase is related to the number of azobenzene units present in the *cis* form and the difference between the free energy gained by insertion of either the *trans* form (negative) or the *cis* form (positive) to the tubular structure. Experimental quantification of this strain energy and its use to produce directional work is ongoing. Ultimately, this system shows potential toward transducing the mechanical action of photoswitches across length scales, as in the process of vision, where large geometrical changes associated with double-bond isomerization are phototransduced by supramolecular assemblies, to yield macroscopic phenomena. We envision that in the future such synthetic molecular self-assembled architectures will be capable of generating directional forces at the nanoscale (e.g., by deformation of vesicular walls).

Materials and Methods

Details of materials, instruments, and methods are provided in *SI Appendix*, including synthesis and characterization of the compounds, optical spectroscopy measurements, DLS, TEM, cryo-TEM, AFM, determination of the critical aggregation concentration, and computational calculation methods. Measurement of length and diameter of the tubules in AFM, TEM, and cryo-TEM images was done using ImageJ 1.46 software.

ACKNOWLEDGMENTS. This work was supported by Netherlands Organization for Scientific Research NWO Project 726.011.001 and European Research Council Starting Grant Phelix (to N.K.). D.B. and G.M.P. acknowledge Swiss National Science Foundation Grant 200021_162827 (to G.M.P.).

1. Kinbara K, Aida T (2005) Toward intelligent molecular machines: Directed motions of biological and artificial molecules and assemblies. *Chem Rev* 105:1377–1400.
2. Abendroth JM, Bushuyev OS, Weiss PS, Barrett CJ (2015) Controlling motion at the nanoscale: Rise of the molecular machines. *ACS Nano* 9:7746–7768.
3. Feringa BL, Browne WR (2011) *Molecular Switches* (Wiley-VCH, Weinheim, Germany), 2nd Ed.
4. Qian H, Wang YY, Guo DS, Aprahamian I (2017) Controlling the isomerization rate of an azo-BF2 switch using aggregation. *J Am Chem Soc* 139:1037–1040.
5. Muraoka T, Kinbara K, Kobayashi Y, Aida T (2003) Light-driven open-close motion of chiral molecular scissors. *J Am Chem Soc* 125:5612–5613.
6. Koumura N, Zijlstra RWJ, van Delden RA, Harada N, Feringa BL (1999) Light-driven monodirectional molecular rotor. *Nature* 401:152–155.
7. Wilson MR, et al. (2016) An autonomous chemically fuelled small-molecule motor. *Nature* 534:235–240.
8. Kassem S, et al. (2017) Artificial molecular motors. *Chem Soc Rev* 46:2592–2621.
9. Anelli PL, Spencer N, Stoddart JF (1991) A molecular shuttle. *J Am Chem Soc* 113: 5131–5133.
10. Bissell RA, Cordova E, Kaifer AE, Stoddart JF (1994) A chemically and electrochemically switchable molecular shuttle. *Nature* 369:133–137.
11. Jiménez MC, Dietrich-Buchecker C, Sauvage JP (2000) Towards synthetic molecular muscles: Contraction and stretching of a linear rotaxane dimer. *Angew Chem Int Ed Engl* 39:3284–3287.
12. von Delius M, Leigh DA (2011) Walking molecules. *Chem Soc Rev* 40:3656–3676.
13. Kassem S, Lee ATL, Leigh DA, Markevicius A, Solà J (2016) Pick-up, transport and release of a molecular cargo using a small-molecule robotic arm. *Nat Chem* 8:138–143.
14. Lewandowski B, et al. (2013) Sequence-specific peptide synthesis by an artificial small-molecule machine. *Science* 339:189–193.
15. Kudernac T, et al. (2011) Electrically driven directional motion of a four-wheeled molecule on a metal surface. *Nature* 479:208–211.
16. Astumian RD (2007) Design principles for Brownian molecular machines: How to swim in molasses and walk in a hurricane. *Phys Chem Chem Phys* 9:5067–5083.
17. Yoshida M, Muneyuki E, Hisabori T (2001) ATP synthase–A marvellous rotary engine of the cell. *Nat Rev Mol Cell Biol* 2:669–677.
18. Mofrad MRK, Kamm RD (2006) *Cytoskeletal Mechanics: Models and Measurements in Cell Mechanics* (Cambridge Univ Press, Cambridge, UK), pp 1–18.
19. Howard J, Hyman AA (2003) Dynamics and mechanics of the microtubule plus end. *Nature* 422:753–758.
20. Grishchuk EL, Molodtsov MI, Ataullakhanov FI, McIntosh JR (2005) Force production by disassembling microtubules. *Nature* 438:384–388.
21. Koshland DE, Mitchison TJ, Kirschner MW (1988) Polewards chromosome movement driven by microtubule depolymerization in vitro. *Nature* 331:499–504.
22. Molodtsov MI, Grishchuk EL, Efremov AK, McIntosh JR, Ataullakhanov FI (2005) Force production by depolymerizing microtubules: A theoretical study. *Proc Natl Acad Sci USA* 102:4353–4358.
23. Kim HJ, et al. (2010) Self-dissociating tubules from helical stacking of noncovalent macrocycles. *Angew Chem Int Ed Engl* 49:8471–8475.
24. Huang Z, et al. (2012) Pulsating tubules from noncovalent macrocycles. *Science* 337: 1521–1526.
25. Albertazzi L, et al. (2014) Probing exchange pathways in one-dimensional aggregates with super-resolution microscopy. *Science* 344:491–495.
26. Yagai S, et al. (2014) Photocontrol over self-assembled nanostructures of π-π stacked dyes supported by the parallel conformer of diarylethene. *Angew Chem Int Ed Engl* 53:2602–2606.
27. Boekhoven J, et al. (2010) Dissipative self-assembly of a molecular gelator by using a chemical fuel. *Angew Chem Int Ed Engl* 49:4825–4828.
28. Krieg E, Bastings MMC, Besenius P, Rybtchinski B (2016) Supramolecular polymers in aqueous media. *Chem Rev* 116:2414–2477.
29. Boekhoven J, Hendriksen WE, Koper GJM, Eelkema R, van Esch JH (2015) Transient assembly of active materials fueled by a chemical reaction. *Science* 349:1075–1079.
30. Sorrenti A, Leira-Iglesias J, Sato A, Hermans TM (2017) Non-equilibrium steady states in supramolecular polymerization. *Nat Commun* 8:15899.
31. Korevaar PA, et al. (2012) Pathway complexity in supramolecular polymerization. *Nature* 481:492–496.
32. De Greef TFA, et al. (2009) Supramolecular polymerization. *Chem Rev* 109:5687–5754.
33. Fuertes A, Juanes M, Granja JR, Montenegro J (2017) Supramolecular functional assemblies: Dynamic membrane transporters and peptide nanotubular composites. *Chem Commun (Camb)* 53:7861–7871.
34. Wang Y, Huang Z, Kim Y, He Y, Lee M (2014) Guest-driven inflation of self-assembled nanofibers through hollow channel formation. *J Am Chem Soc* 136:16152–16155.
35. Chen CJ, Liu GY, Liu XS, Li DD, Ji J (2012) Construction of photo-responsive micelles from azobenzene-modified hyperbranched polyphosphates and study of their reversible self-assembly and disassembly behaviours. *New J Chem* 36:694–701.
36. Smulders MMJ, Schenning APHJ, Meijer EW (2008) Insight into the mechanisms of cooperative self-assembly: The "sergeants-and-soldiers" principle of chiral and achiral C3-symmetrical discotic triamides. *J Am Chem Soc* 130:606–611.
37. Pescitelli G, Di Bari L, Berova N (2014) Application of electronic circular dichroism in the study of supramolecular systems. *Chem Soc Rev* 43:5211–5233.
38. Bochicchio D, Salvalaglio M, Pavan GM (2017) Into the dynamics of a supramolecular polymer at submolecular resolution. *Nat Commun* 8:147.
39. Barducci A, Bussi G, Parrinello M (2008) Well-tempered metadynamics: A smoothly converging and tunable free-energy method. *Phys Rev Lett* 100:020603.
40. Baker MB, et al. (2015) Consequences of chirality on the dynamics of a water-soluble supramolecular polymer. *Nat Commun* 6:6234.